

## Highly efficient non-degenerate four-wave mixing under dual-mode injection in InP/InAs quantum-dash and quantum-dot lasers at 1.55 $\mu\text{m}$

T. Sadeev, H. Huang, D. Arsenijević, K. Schires, F. Grillot, and D. Bimberg

Citation: *Applied Physics Letters* **107**, 191111 (2015); doi: 10.1063/1.4935796

View online: <http://dx.doi.org/10.1063/1.4935796>

View Table of Contents: <http://scitation.aip.org/content/aip/journal/apl/107/19?ver=pdfcov>

Published by the [AIP Publishing](#)

---

### Articles you may be interested in

[Non-degenerate four-wave mixing in an optically injection-locked InAs/InP quantum dot Fabry–Perot laser](#)  
*Appl. Phys. Lett.* **106**, 143501 (2015); 10.1063/1.4916738

[15 Gb/s index-coupled distributed-feedback lasers based on 1.3  \$\mu\text{m}\$  InGaAs quantum dots](#)  
*Appl. Phys. Lett.* **105**, 011103 (2014); 10.1063/1.4887063

[Time-resolved chirp in an InAs/InP quantum-dash optical amplifier operating with 10 Gbit/s data](#)  
*Appl. Phys. Lett.* **87**, 021104 (2005); 10.1063/1.1994947

[Nonlinear processes responsible for nondegenerate four-wave mixing in quantum-dot optical amplifiers](#)  
*Appl. Phys. Lett.* **77**, 1753 (2000); 10.1063/1.1311319

[High-frequency properties of 1.55  \$\mu\text{m}\$  laterally complex coupled distributed feedback lasers fabricated by focused-ion-beam lithography](#)  
*Appl. Phys. Lett.* **77**, 325 (2000); 10.1063/1.126965

---

The logo for Applied Physics Reviews (AIP) is shown in white text on an orange background. The background features a pattern of wavy, light-colored lines. To the left of the logo is a small image of the journal cover, which includes a diagram of a quantum dot structure and a graph.

**NEW Special Topic Sections**

**NOW ONLINE**  
Lithium Niobate Properties and Applications:  
Reviews of Emerging Trends

**AIP** Applied Physics Reviews



## Highly efficient non-degenerate four-wave mixing under dual-mode injection in InP/InAs quantum-dash and quantum-dot lasers at 1.55 $\mu\text{m}$

T. Sadeev,<sup>1,a)</sup> H. Huang,<sup>2</sup> D. Arsenijević,<sup>1</sup> K. Schires,<sup>2</sup> F. Grillot,<sup>2,3</sup> and D. Bimberg<sup>1,4</sup>

<sup>1</sup>*Institut für Festkörperphysik, Technische Universität Berlin, Berlin 10623, Germany*

<sup>2</sup>*Télécom Paristech, Université Paris-Saclay, 46 rue Barrault, CNRS LTCI 75634 Paris Cedex 13, France*

<sup>3</sup>*Center for High Technology Materials, University of New-Mexico, Albuquerque, New Mexico 1313, USA*

<sup>4</sup>*King Abdulaziz University, 22254 Jeddah, Saudi Arabia*

(Received 18 August 2015; accepted 3 November 2015; published online 13 November 2015)

This work reports on non-degenerate four-wave mixing under dual-mode injection in metalorganic vapor phase epitaxy grown InP/InAs quantum-dash and quantum dot Fabry-Perot laser operating at 1550 nm. High values of normalized conversion efficiency of  $-18.6$  dB, optical signal-to-noise ratio of 37 dB, and third order optical susceptibility normalized to material gain  $\chi^{(3)}/g_0$  of  $\sim 4 \times 10^{-19} \text{ m}^3/\text{V}^3$  are measured for 1490  $\mu\text{m}$  long quantum-dash lasers. These values are similar to those obtained with distributed-feedback lasers and semiconductor optical amplifiers, which are much more complicated to fabricate. On the other hand, due to the faster gain saturation and enhanced modulation of carrier populations, quantum-dot lasers demonstrate 12 dB lower conversion efficiency and 4 times lower  $\chi^{(3)}/g_0$  compared to quantum dash lasers. © 2015 AIP Publishing LLC.

[<http://dx.doi.org/10.1063/1.4935796>]

Most semiconductor based devices exhibit strong nonlinearities, making them very attractive for applications based on four-wave mixing (FWM). Amongst them, modulation format transparent wavelength conversion, submillimetre wave generation, and optical signal processing are of largest importance.<sup>1,2</sup> FWM is driven by the third order optical susceptibility  $\chi^{(3)}$  (Ref. 3) as already observed in semiconductor optical amplifiers (SOA), whose large linear gain is advantageous to generate high power beat-products for weak pump and signal.<sup>4,5</sup> Another approach can be obtained via distributed feedback lasers (DFB), where the lasing mode acts as a pump.<sup>6</sup> Already in the 1985–1990s,<sup>7–11</sup> Fabry-Perot (F-P) lasers were originally used to generate FWM; however, those do usually suffer from a low conversion efficiency and succeed only for a relatively low frequency detuning of a few tens of GHz. The advent of nanostructure based light emitters (quantum-dot/quantum-dash lasers)<sup>12,13</sup> has resumed the interest to this topic due to their higher nonlinear gain, low injection currents, ultra-fast carrier dynamics, low ASE, and broad gain spectrum.<sup>14–17</sup> As already reported, depending on the crystal growth conditions, both types of nanostructures with similar features, such as large gain, inhomogeneously broadened gain spectra, and high characteristic temperature, can be obtained for the same wavelength range.<sup>11,12,17</sup> For instance, quantum dashes, which are electronically elongated dots with a larger volume, do have a larger density of close lying delta function states contributing to efficient FWM,<sup>18</sup> and which result in a larger difference between values of  $\chi^{(3)}$  between quantum-dash (QDash) and quantum-dot (QDot) lasers as reported here. An experimental comparative study of FWM in QDash and QDot F-P lasers at 1550 nm has not been yet presented. To this end, this letter presents a comprehensive comparison of FWM in QDot and QDash lasers shedding the light on which structural approach should be

considered for applications (e.g., wavelength conversion, microwave signal generation, etc.). In particular, our comparison between QDot and QDash devices shows promising large non-linear interaction comparable to DFBs and SOAs.<sup>19,20</sup>

The laser structures used in this work are grown by MOVPE on n-type (001) InP substrate. The active layer consists of 7 stacked QDash (QDot) layers in an  $\text{In}_{0.78}\text{Ga}_{0.22}\text{As}_{0.47}\text{P}_{0.53}$  matrix, enclosed by an  $\text{In}_{0.82}\text{Ga}_{0.18}\text{As}_{0.40}\text{P}_{0.60}$  waveguide. Laterally, single-mode laser buried heterostructures are formed by deep etching through the active region and regrowth of p/n-blocking and contact layers. The temperature of growth and the indium flux rate decide the type of nanostructure (QDot or QDash) formed. Details of material growth, processing and results of material characterisation are found in Ref. 21. We investigate here two groups of devices: QDash and QDot lasers with similar cavity lengths around 750  $\mu\text{m}$  and longer devices with cavities of 1490  $\mu\text{m}$  and 1250  $\mu\text{m}$  for the QDash and QDot, respectively. The first group with shorter cavity is only used to compare the maximum achievable FWM efficiency for lasers with the same dimensions. The longer devices, offering a longer interaction length, are the main devices studied in this article. The ridge width is 1  $\mu\text{m}$ , and no coating is applied to the facets of the devices. The laser bars are mounted on copper blocks for higher thermo-electrical conductivity and fixed on a plate with thermoelectric control. Light-current curves measured at room temperature are shown in Fig. 1 for both the QDash and QDot devices, showing threshold currents of about 24 mA and 19 mA and slope efficiencies of 19% and 28%, respectively. The turn-on voltage is 0.8 V for both devices; the series resistance  $R_s$ , measured at  $2.5 \times I_{\text{thr}}$ , is 5.1  $\Omega$  and 3.7  $\Omega$  for the QDash and Qdot lasers, respectively. Net gain spectra of the devices as a function of current are measured from the spontaneous emission spectra and presented in Fig. 2. The asymmetry in the net gain profiles is most

<sup>a)</sup>Electronic mail: tagir@mailbox.tu-berlin.de

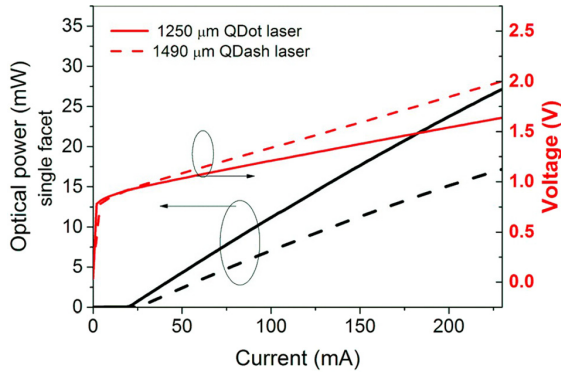


FIG. 1. LIV-characteristics.

probably due to slightly lower population of higher energy levels (shorter wavelengths) as well as to the width of the inhomogeneously broadened spectrum, which is of about 40 nm at 23 and 20 mA, respectively, both for QDash and QDot lasers.

The most common way of investigating FWM in semiconductor lasers is based on a pump/probe configuration. In this work, the pump laser is used as a master laser to lock a longitudinal mode at the gain peak of the slave F-P laser. Depending on the two degrees of freedom of optical injection, the detuning between the master and slave and the master laser power, the slave F-P laser can either be unaffected by the injection, oscillating in a periodic or aperiodic fashion, or be injection-locked to the master and emit a single mode resonant to the injected signal.<sup>22</sup> In this work, the slave lasers are injection-locked using a ratio between the optical power of the master and slave lasers of 1 dB, and detunings such that the slave lasers operate well within the injection-locking range. Spectra for both lasers under free running (FR) and injection-locked (IL) operations are shown in Fig. 3. We note that both free running QDot and QDash lasers show inhomogeneously broadened spectra with FWHM (full-width at half maximum) of 3.2 nm. The probe signal, with a power 3 dB below that of the free running laser, is then swept from shorter to longer wavelengths around the locked mode. Fig. 4 shows optical spectra for a QDot laser under this dual-injection, with the probe laser tuned to longer

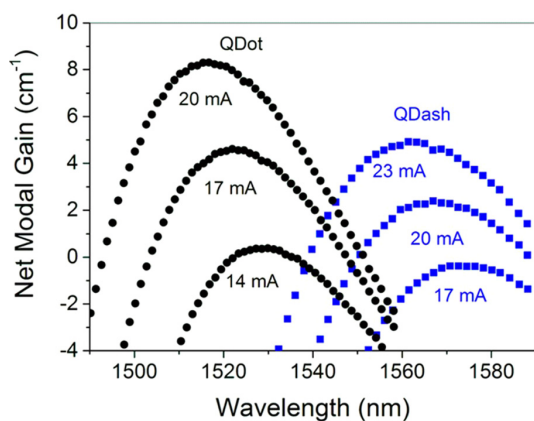
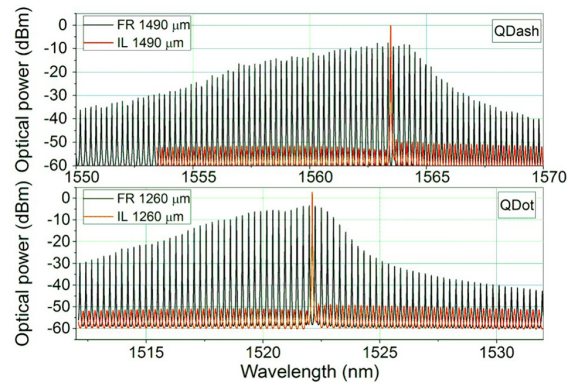


FIG. 2. Net gain spectra below threshold.

FIG. 3. Optical spectra at 2.5  $I_{th}$ : FR-free running laser; IL-injection locked laser.

wavelengths. The positively detuned FWM-signal is marked as “Probe conversion.”

The subsequent measurement techniques employed are similar to those reported in Ref. 23. Normalized conversion efficiency (NCE), defined as

$$NCE = \frac{Power_{FWM}}{Power_{PROBE} Power_{PUMP}^2} \quad [mW^{-2}] \quad (1)$$

along with optical signal-to-noise ratio (OSNR) results are shown in Fig. 5. NCE values are given in dB and correspond to  $10\log_{10}(NCE/1 mW^{-2})$ . A maximum NCE of  $-18.6$  dB is measured for the QDash laser, being 12 dB larger than the QDot laser. The QDash device also demonstrates a broader frequency detuning range from  $-1.2$  to  $2.7$  THz. Owing to the optical injection, very large OSNRs of 37 dB at 27 GHz and 22 dB at 67 GHz detuning are measured for QDash and QDot lasers, respectively. Remarkably, it is very important to stress that these values are comparable with those measured for more complex DFB-laser structures,<sup>24</sup> bulk and Qdash/Qdot SOA's,<sup>4,20</sup> and larger than values previously reported for InAs/InP QDot lasers.<sup>19,23</sup>

The larger NCE observed at positive detuning ( $\lambda_{pump} < \lambda_{probe}$ ) and for both devices is attributed to the asymmetric gain profiles (Fig. 2) and the wavelength dependence of the alpha factor (Fig. 6). For detunings above

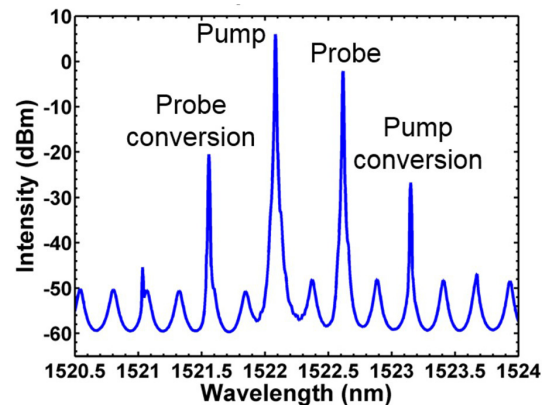


FIG. 4. Optical spectra of QD laser under dual-mode injection at 50 mA current.

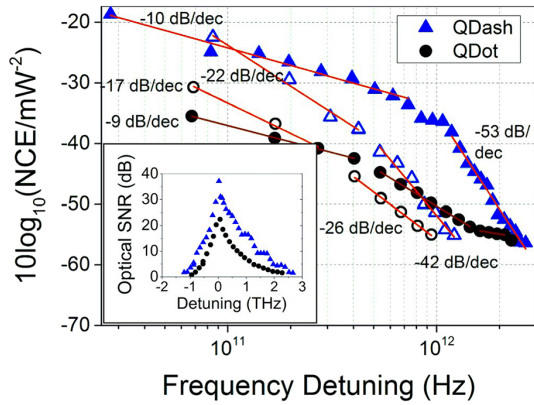


FIG. 5. Nonlinear conversion efficiency (solid/empty scatter–positive/negative detuning, respectively) and optical SNR (inset).

400 GHz, the larger alpha factor measured for QDash lasers leads to a difference of  $\sim 10$  dB between “positive” and “negative” NCE while the latter is reduced down to 5 dB for QDot lasers, owing to the reduced phase-amplitude coupling. The NCE found for positively detuned QDash lasers resembles the results already published for QDash SOAs.<sup>25</sup> Two regions are distinguished: a first decrease in 10 dB/decade, followed by a faster decrease in 53 dB/decade. The first region has a picosecond characteristic time, controlled by an efficient interband carrier-density pulsation (CDP) process.<sup>26</sup> The rapid decrease with 53 dB/decade starting at 1 THz represents the joint, but de-phased effects of different dynamic processes: CDP, carrier heating and spectral hole burning<sup>27</sup> with a sub-picosecond characteristic time. Qualitatively, this behaviour is also similar for QDot lasers, which show a lower conversion efficiency most likely due to the phonon bottleneck combined to the lower modulation amplitude of carrier population arising from a reduced number of active states. The former is known to restrain the coupling of carriers between spatially isolated quantum dots and the surrounding material with large energy spacing.<sup>28</sup> However, in case of QDashes, the carriers are captured from the bulk or QW surrounding areas into the numerous overlapping states

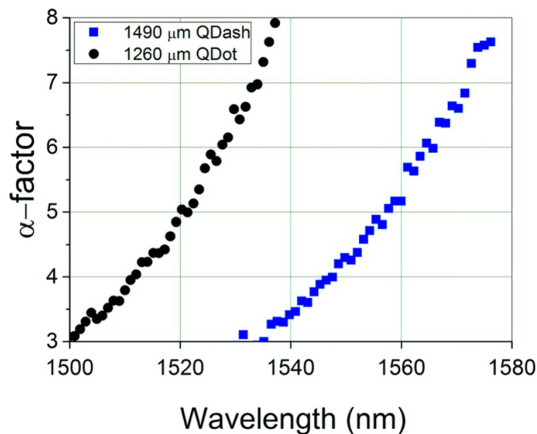


FIG. 6. Dependence of  $\alpha$ -factor on wavelength for QDot and QDash lasers.

with the same transition energies of the dash DOS function.<sup>28</sup> Two-photon absorption phenomenon (TPA) may also be decisive since the latter was proved to stimulate ultra-fast gain recovery in QDash SOAs at energies above and below the pump.<sup>29</sup> The flattening of the NCE-curve observed for a positively detuned probe around 1 THz in the case of the QDash device may result from this phenomenon. Thus, the QDash DOS, which consists of many overlapping inhomogeneously broadened states with high energy tail, may favour additional gain at the FWM-signal wavelengths and leads to a larger FWM-conversion efficiency.<sup>18</sup> Although a higher FWM efficiency is naturally expected from a longer interaction length,<sup>4</sup> it is important to stress that OSNR and NCE of devices with cavity length of  $750 \mu\text{m}$  are, respectively, found to be 12 and 5.2 dB larger for QDash compared to QDot ones.

The conversion efficiency for both QDash and QDot devices remains below  $-55$  dBm and nearly equal for large positive  $f > 2$  THz and negative  $f > 1$  THz detuning (Fig. 5). This indicates that pump-probe detuning exceeds the bandwidth where the conversion is fast and effective. In this region, QDash lasers demonstrate a rapid decrease of 53 dB/decade, whereas QDot rolls off at 21 dB/decade. The low NCE in this detuning region can be attributed to the smaller number of QDashes/QDots occupied by excitons, since the density of nanostructures in these wavelength regions of the gain spectra is lower. To this end, the abrupt gain spectra profile can explain the equalization of QDash and Qdot NCE at lower negative detuning. Finally, carrier dynamics in quantum dashes also may suffer from a phonon bottleneck when the energy spacing is large. The third-order optical susceptibility normalized to optical linear gain  $\chi^{(3)}/g_0$  is calculated using the formula from Ref. 6 and assuming an effective mode area of  $1.3 \mu\text{m}^2$ ,

$$NCE = \left| \frac{3k_0}{4n} \Gamma \chi^{(3)} \frac{\exp\left(\frac{\Gamma g L}{2}\right) - 1}{\Gamma g} \right|^2. \quad (2)$$

The value of  $\chi^{(3)}/g_0$  decreases from  $4 \times 10^{-19} \text{ m}^3/\text{V}^3$  down to  $6.0 \times 10^{-21} \text{ m}^3/\text{V}^3$  in the 0.027–2.66 THz detuning range for QDash lasers and from  $9.4 \times 10^{-20} \text{ m}^3/\text{V}^3$  to  $5.1 \times 10^{-21} \text{ m}^3/\text{V}^3$  in 0.068–2.270 THz range for QDot lasers. Remarkably, the  $\chi^{(3)}/g_0$  value for the QDash gain medium is larger than the one measured for DFB lasers<sup>6</sup> and references therein.

In conclusion, we have observed a unique and large normalized conversion efficiency of  $-18.6$  dB, OSNR of 37 dB, and a conversion achievable for frequency detunings up to 3 THz in MOVPE-grown  $1490 \mu\text{m}$ -long InP/InAs quantum-dash lasers operating at 1550 nm under dual-mode optical injection. These values are the highest reported for F-P lasers and comparable to ones reported for DFB-lasers and SOAs more complex to process. We observe a larger conversion efficiency for  $1490 \mu\text{m}$ -long QDash devices in comparison to  $1250 \mu\text{m}$ -long QDot lasers, fabricated by the same growth and processing techniques. QDot devices with delta-function DOS show a four times lower third-order optical susceptibility, a 12 dB-lower normalized conversion efficiency and



14.7 dB-lower optical signal-to-noise ratio. The analysis confirms that such a difference is not only due to the cavity length but also to additive contributions to the gain such as TPA, faster gain saturation, and enhanced modulation of carrier populations.

The authors thank D. Franke and J. Kreissl for material growth and device processing. T.S. is thankful to Collaborative Research Centre 787 (SFB 787) of Deutsche Forschungsgemeinschaft and Seventh Framework Programme through PROPHET Initial Training Network. F.G., K.S., and H.H. acknowledge Campus France for financial support as well as the Futur & Ruptures program and the French National Research Agency (ANR) through the Nanodesign Project funded by the IDEX Paris-Saclay, ANR-11-IDEX-0003-02.

- <sup>1</sup>T. Chattopadhyay, "Submillimeter wave generation through optical four-wave mixing using injection-locked semiconductor lasers," *J. Lightwave Technol.* **20**(3), 502–506 (2002).
- <sup>2</sup>D. F. Geraghty, R. B. Lee, M. Verdiell, M. Ziari, A. Mathur, and K. J. Vahala, "Wavelength conversion for WDM communication systems using four-wavemixing in semiconductor optical amplifiers," *IEEE J. Sel. Top. Quantum Electron.* **3**(5), 1146–1155 (1997).
- <sup>3</sup>M. Sugawara, *Self-Assembled InGaAs/GaAs Quantum Dots* (Academic Press, 1999).
- <sup>4</sup>A. D'Ottavi, F. Girardin, L. Graziani, F. Martelli, P. Spano, A. Mecozzi, S. Scotti, R. Dall'Ara, J. Eckner, and G. Guekos, "Four-wave mixing in semiconductor optical amplifiers: A practical tool for wavelength conversion," *IEEE J. Sel. Top. Quantum Electron.* **3**(2), 522–528 (1997).
- <sup>5</sup>K. Kikuchi, M. Kakui, C. Zah, and T. Lee, "Observation of highly nondegenerate four-wave mixing in 1.5  $\mu\text{m}$  traveling-wave semiconductor optical amplifiers and estimation of nonlinear gain coefficient," *IEEE J. Quantum Electron.* **28**(1), 151–156 (1992).
- <sup>6</sup>H. Su, H. Li, L. Zhang, Z. Zou, A. L. Gray, R. Wang, P. M. Varangis, and L. F. Lester, "Nondegenerate four-wave mixing in quantum dot distributed feedback lasers," *IEEE Photonics Technol. Lett.* **17**(8), 1686–1688 (2005).
- <sup>7</sup>H. Nakajima and R. Frey, "Observation of bistable reflectivity of a phase-conjugated signal through intracavity nearly degenerate four-wave mixing," *Phys. Rev. Lett.* **54**(16), 1798–1801 (1985).
- <sup>8</sup>J.-M. Liu and T. B. Simpson, "Four-wave mixing and optical modulation in a semiconductor laser," *IEEE J. Quantum Electron.* **30**(4), 957–965 (1994).
- <sup>9</sup>S. Jiang and M. Dagenais, "Nearly degenerate four-wave mixing in Fabry-Perot semiconductor lasers," *Opt. Lett.* **18**(16), 1337 (1993).
- <sup>10</sup>R. Nietzke, P. Panknin, W. Elsaesser, and E. O. Goebel, "Four-wave mixing in GaAs/AlGaAs semiconductor lasers," *IEEE J. Quantum Electron.* **25**(6), 1399–1406 (1989).
- <sup>11</sup>G. Agrawal, "Four-wave mixing and phase conjugation in semiconductor laser media," *Opt. Lett.* **12**(4), 260–262 (1987).
- <sup>12</sup>D. Bimberg, "Quantum dot based nanophotonics and nanoelectronics," *Electron. Lett.* **44**(3), 168–171 (2008).
- <sup>13</sup>D. Bimberg, N. Kirstaedter, N. Ledentsov, Z. Alferov, P. Kop'ev, and V. Ustinov, "InGaAs-GaAs quantum-dot lasers," *IEEE J. Sel. Top. Quantum Electron.* **3**(2), 196–205 (1997).
- <sup>14</sup>O. Shchekin and D. Deppe, "1.3  $\mu\text{m}$  InAs quantum dot laser with  $T_0 = 161$  K from 0 to 80 °C," *Appl. Phys. Lett.* **80**(18), 3277–3279 (2002).
- <sup>15</sup>R. L. Sellin, C. Ribbat, M. Grundmann, N. N. Ledentsov, and D. Bimberg, "Close-to-ideal device characteristics of high-power InGaAs/GaAs quantum dot lasers," *Appl. Phys. Lett.* **78**(9), 1207–1209 (2001).
- <sup>16</sup>O. Karni, K. J. Kuchar, A. Capua, V. Mikhelashvili, G. Sek, J. Misiewicz, V. Ivanov, J. P. Reithmaier, and G. Eisenstein, "Carrier dynamics in inhomogeneously broadened InAs/AlGaInAs/InP quantum-dot semiconductor optical amplifiers," *Appl. Phys. Lett.* **104**(12), 121104 (2014).
- <sup>17</sup>J. Gomis-Bresco, S. Dommers-Völkel, O. Schöpfs, Y. Kaptan, O. Dyatlova, D. Bimberg, and U. Woggon, "Time-resolved amplified spontaneous emission in quantum dots," *Appl. Phys. Lett.* **97**(25), 251106 (2010).
- <sup>18</sup>H. Dery, E. Benisty, A. Epstein, R. Alizon, V. Mikhelashvili, G. Eisenstein, R. Schwertberger, D. Gold, J. P. Reithmaier, and A. Forchel, "On the nature of quantum dash structures," *J. Appl. Phys.* **95**(11), 6103–6111 (2004).
- <sup>19</sup>H. Huang, K. Schires, P. J. Poole, and F. Grillot, "Non-degenerate four-wave mixing in an optically injection-locked InAs/InP quantum dot Fabry-Perot laser," *Appl. Phys. Lett.* **106**(14), 143501 (2015).
- <sup>20</sup>Z. Lu, J. Liu, S. Raymond, P. Poole, P. Barrios, D. Poitras, F. Sun, G. Pakulski, P. Bock, and T. Hall, "Highly efficient non-degenerate four-wave mixing process in InAs/InGaAsP quantum dots," *Electron. Lett.* **42**(19), 1112–1114 (2006).
- <sup>21</sup>D. Franke, J. Kreissl, W. Rehbein, F. Wenning, H. Kuenzel, U. Pohl, and D. Bimberg, "Effect of the shape of InAs nanostructures on the characteristics of InP-based buried heterostructure semiconductor optical amplifiers," *Appl. Phys. Express* **4**(1), 014101 (2011).
- <sup>22</sup>T. B. Simpson, J. M. Liu, K. F. Huang, and K. Tai, "Nonlinear dynamics induced by external optical injection in semiconductor lasers," *Quantum Semiclassical Opt.* **9**(5), 765–784 (1999).
- <sup>23</sup>C. Wang, F. Grillot, F.-Y. Lin, I. Aldaya, T. Batte, C. Gosset, E. Decerle, and J. Even, "Nondegenerate four-wave mixing in a dual-mode injection-locked InAs/InP(100) nanostructure laser," *IEEE Photonics J.* **6**(1), 1–8 (2014).
- <sup>24</sup>H. Su and L. F. Lester, "Dynamic properties of quantum dot distributed feedback lasers: High speed, linewidth and chirp," *J. Phys. D: Appl. Phys.* **38**, 2112–2118 (2005).
- <sup>25</sup>A. Bilenca, R. Alizon, V. Mikhelashvili, D. Dahan, G. Eisenstein, R. Schwertberger, D. Gold, J.-P. Reithmaier, and A. Forchel, "Broad-band wavelength conversion based on cross-gain modulation and four-wave mixing in InAs-InP quantum-dash semiconductor optical amplifiers operating at 1550 nm," *IEEE Photonics Technol. Lett.* **15**(4), 563–565 (2003).
- <sup>26</sup>G. Agrawal, "Population pulsations and nondegenerate four-wave mixing in semiconductor lasers and amplifiers," *J. Opt. Soc. Am. B* **5**(1), 147 (1988).
- <sup>27</sup>O. Karni, A. Capua, G. Eisenstein, D. Franke, J. Kreissl, H. Kuenzel, D. Arsenijević, H. Schmeckeber, M. Stubenrauch, M. Kleinert, D. Bimberg, C. Gilfert, and J. P. Reithmaier, "Nonlinear pulse propagation in a quantum dot laser," *Opt. Express* **21**(5), 5715–5736 (2013).
- <sup>28</sup>H. Dery and G. Eisenstein, "Self-consistent rate equations of self-assembly quantum wire lasers," *IEEE J. Quantum Electron.* **40**(10), 1398–1409 (2004).
- <sup>29</sup>A. Capua, G. Eisenstein, and J. P. Reithmaier, "A nearly instantaneous gain response in quantum dash based optical amplifiers," *Appl. Phys. Lett.* **97**(13), 131108 (2010).